$( )^T$ = transpose
∇ = gradient operator
$\mathfrak{d}/\mathfrak{d}t$ = Oldroyd differential operator

LITERATURE CITED

Acierno, D., et al., "Rheological and Heat Transfer Aspects of the Melt Spinning of Monofilament Fibers of Polyethylene and Polystyrene," *J. Appl. Poly. Sci.*, **15**, 2395 (1971).

Baid, K. M., "Elongational Flows of Dilute Polymer Solutions," Ph.D. dissertation, Univ. Delaware, Newark (1973).

Chen, I.-J., et al., "Interpretation of Tensile and Melt Spinning Experiments on Low Density and High Density Polyethylene," *Trans. Soc. Rheol.*, **16**, 473 (1972).

Denn, M. M., *Stability of Reaction and Transport Processes*, Prentice-Hall, Englewood Cliffs, N. J. (1975).

———., and G. Marrucci, "Stretching of Viscoelastic Liquids," *AIChE J.*, **17**, 101 (1971).

Kanel, F., "The Extension of Viscoelastic Materials," Ph.D. dissertation, Univ. Delaware, Newark (1972).

Matovich, M. A., and J. R. A. Pearson, "Spinning a Molten Threadline: Steady State, Isothermal Viscous Flows," *Ind. Eng. Chem. Fundamentals*, **8**, 512 (1968).

Metzner, A. B., et al., "Behavior of Viscoelastic Materials in Short-Time Processes," *Chem. Eng. Progr.*, **62** (12), 81 (1966).

Mewis, J., and A. B. Metzner, "The Rheological Properties of Suspensions of Fibres in Newtonian Fluids Subject to Extensional Deformations," *J. Fluid Mech.*, **62**, 593 (1974).

Pearson, J. R. A., and M. A. Matovich, "Spinning a Molten Threadline: Stability," *Ind. Eng. Chem. Fundamentals*, **8**, 605 (1969).

Petrie, C. J. S., "Memory Effects in a Non-Uniform Flow: A Study of the Behavior of a Tubular Film of Viscoelastic Fluid," *Rheol. Acta*, **12**, 92 (1973).

Spearot, J. A., "The Isothermal Spinning of Molten Polyethylenes," Ph.D. dissertation, Univ. Delaware, Newark (1972).

———., and A. B. Metzner, "Isothermal Spinning of Molten Polyethylenes," *Trans. Soc. Rheol.*, **16**, 495 (1972).

Sun, Z.-S., and M. M. Denn, "Stability of Rotational Couette Flow of Polymer Solutions," *AIChE J.*, **18**, 1010 (1972).

Weinberger, C. B., and J. D. Goddard, "Extensional Flow Behavior of Polymer Solutions and Particle Suspensions in a Spinning Motion, *Intern. J. Multiphase Flow*, **1**, 465 (1974).

Zeichner, G. R., "Spinnability of Viscoelastic Fluids," M.Ch.E. thesis, Univ. Delaware, Newark (1973).

Manuscript received January 2, 1975; revision received March 28 and accepted March 31, 1975.

Real-Time Time-Optimal Control of a Stirred-Tank Reactor Using Kalman Filtering for State Estimation

This paper presents the development and real-time implementation of a time-optimal control algorithm for a continuous stirred-tank reactor. A multivariable time-optimal control law is derived and an Extended Kalman Filter formuated for on-line estimation and filtering. The work demonstrates the powerful capability of real-time computation and decision-making in optimal control and optimal estimation of process states.

EDMOND B. LYNCH
and
W. FRED RAMIREZ
Department of Chemical Engineering
University of Colorado
Boulder, Colorado 80302

SCOPE

With the advent of the process computer and particularly the minicomputer, computer control is beginning to take hold in the chemical industry. Most of this computer control activity, however, has been essentially data acquisition with heavy operator intervention, or on the most sophisticated level, feedback control on isolated states of the process.

In contrast to single-loop feedback control, the implementation of optimal control demands knowledge of all the process states of the system. Although much simulation work has been done using optimal control theory and some experimental work has been demonstrated, little to date has been reported on using on-line digital optimal control for actual nonlinear systems. Thus, the motivation of this work is the development and implementation of a time-optimal control algorithm for a continuously stirred-tank reactor. The reaction studied is the decomposition of hydrogen peroxide. A General Data Corporation Nova 1210 series minicomputer with 8K words of storage was used to implement the time-optimal control policy. Also an Extended Kalman Filter is used to determine optimal estimates of the process states.

CONCLUSIONS AND SIGNIFICANCE

This paper presents a total study of on-line computer control of a chemical process. It takes a well modeled process with realistic systematic noise and measurement difficulty, and controls the process time-optimally without using large amounts of minicomputer core storage. A multivariable time optimal control law is derived and an Extended Kalman Filter formulated for on-line estimation and filtering of the process states. Simulation and experimental results show that the Kalman Filter works very well in estimating the unmeasured system states and filtering the measurement noise in the system. Simulated and experimental trajectories investigated modeling uncertainties between the actual real-time controlled system and a simulated

---

Correspondence concerning this paper should be addressed to W. F. Ramirez.

system under time-optimal control. A comparison of this multivariable time-optimal control policy shows that it is significantly better (faster to reach the desired target set) than either a one variable time-optimal control or multivariable proportional feedback control. This work demonstrates the powerful on-line capability of real-time computation and decision-making in optimal control and optimal estimation of process states.

MATHEMATICAL MODEL

The nonlinear process considered is the decomposition of hydrogen peroxide with a homogeneous catalyst of potassium iodide forming the products of water and oxygen gas. The reaction is carried out in a continuously stirred-tank reactor. Much of the fundamental work for this system as well as an experimental demonstration of time-optimal control using a single control variable of coolant flow was done by Nyquist (1970) and Nyquist and Ramirez (1971). In the present study an additional control variable of the potassium iodide catalyst flow rate was considered. The following equations form the dynamic model:

Peroxide material balance

$$\frac{dC}{dt} = \frac{F_p C_0}{V_x} - \frac{FC}{V_x} - R \qquad (1)$$

Catalyst material balance

$$\frac{dC_{KI}}{dt} = \frac{(F - F_p)}{V_x} C_{KI0} - \frac{C_{KI}}{V_x} \qquad (2)$$

Energy balance

$$\frac{dT}{dt} = \frac{(F_p + F_{KI})(T_0 - T)}{V_H} + \frac{Q_s}{V_H \rho C_p} + \frac{(-\Delta H) R V_x}{V_H \rho C_p} - \frac{\beta (T - T_C)}{V_H \rho C_p} \qquad (3)$$

Reaction rate expression

$$R = k_0\, e^{-E/R'T}\, C_{KI}\, C \qquad (4)$$

An information flow diagram for the complete model is given in Figure 1. Table 1 shows typical steady state and parameter values. Comparison of the model to actual dynamic data shows agreement to within 3% maximum error in system temperature and reaction concentration (Lynch, 1975).

TABLE 1. STEADY STATE AND PARAMETER VALUES

F_p = 750 ml/min
C_0 = 2.25 g moles/liter
V_x = 15.78 liters
C_s = 1.718 g moles/liter
k_0 = 9.775×10^9
C_{KI_s} = .0019 g moles/liter
E/R' = 6524 cal/g mole
T_s = 30°C
F_{KI_s} = 100 ml/min
V_H = 17.36 liters
T_0 = 25°C
a = 1284.6 cal/min
b = −23.61 cal/min °C
b_1 = 1,510 cal/min °C
b_2 = 27.26 cal/min volt °C
b_3 = 0.1499 cal/min volt^2 °C
b_4 = 0.00238 cal/min volt^3 °C
b_5 = −0.489 liter/min
b_6 = 0.03418 liter/min volt
b_7 = -3.584×10^{-4} liter/min volt^2
b_8 = 1.421×10^{-6} liter/min volt^3
β_s = 122.1
ρ = 1 g/cc
C_p = 1 cal/g °C
$(-\Delta H)$ = 22,600 cal/g mole

TABLE 2. STATE VARIABLE FORMULATION

State variables

$$x_1 = \frac{T - T_s}{T_s}$$

$$x_2 = \frac{C - C_s}{C_s}$$

$$x_3 = \frac{C_{KI} - C_{KI_s}}{C_{KI_s}}$$

Control variables

$$u_1 = \frac{\beta - \beta_s}{\beta_s}$$

$$u_2 = \frac{F_{KI} - F_{KI_s}}{F_{KI_s}}$$

Measured variables

$$m_1 = x_1$$

$$m_2 = R - R_s$$

OPTIMAL CONTROL FORMULATION

In state variable formulation, the system has three state variables, two control variables, and two measured variables. Table 2 defines the specific variables. The system dynamics are nonlinear in the state variables and linear in the controls

$$\dot{\mathbf{x}} = \mathbf{g}(\mathbf{x}) + \mathbf{B}(\mathbf{x})\,\mathbf{u} \qquad (5)$$

For time-optimal control to a target set about a desired steady state, Pontryagin's Maximum Principle (Athans and Falb, 1966) states that the Hamiltonian must be maximized. The Hamiltonian for this system under a time-optimal objective function is

$$H = -1 + p_1 f_1 + p_2 f_2 + p_3 f_3 \qquad (6)$$

where f are nonlinear functions given by the model equations

$$\dot{\mathbf{x}} = \mathbf{f}(\mathbf{x}, \mathbf{u}) \qquad (7)$$

and p are the co-state variables defined by

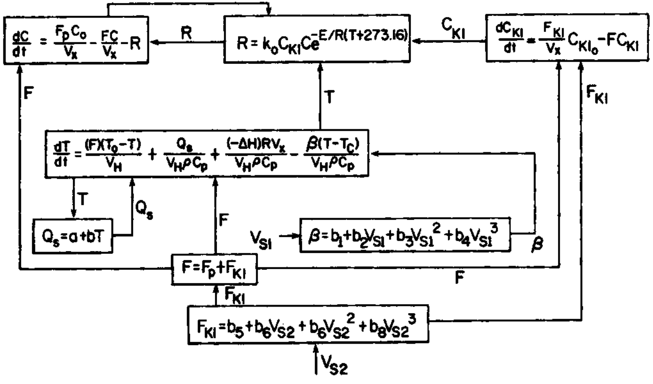

Fig. 1. Information flow diagram for system model.

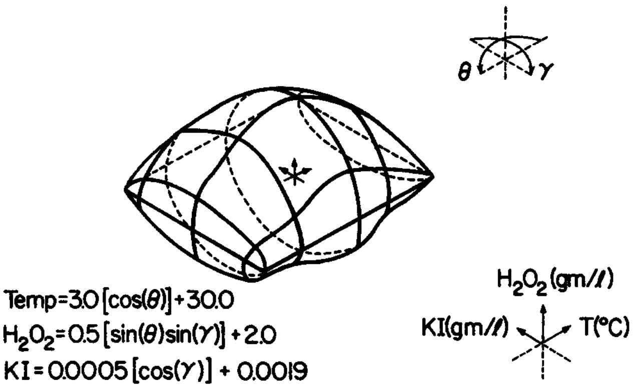

Fig. 2. Three-dimensional view of target set region.

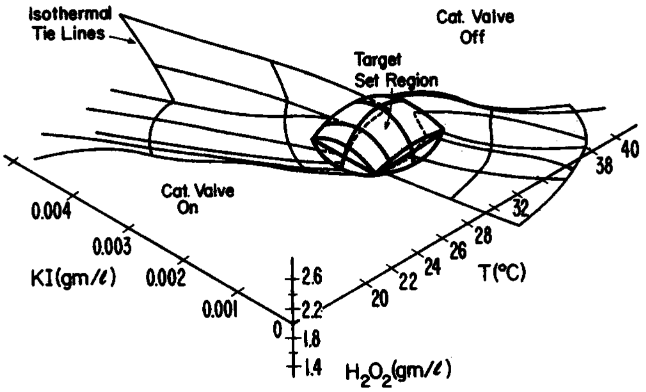

Fig. 3. Catalyst valve switching surfaces.

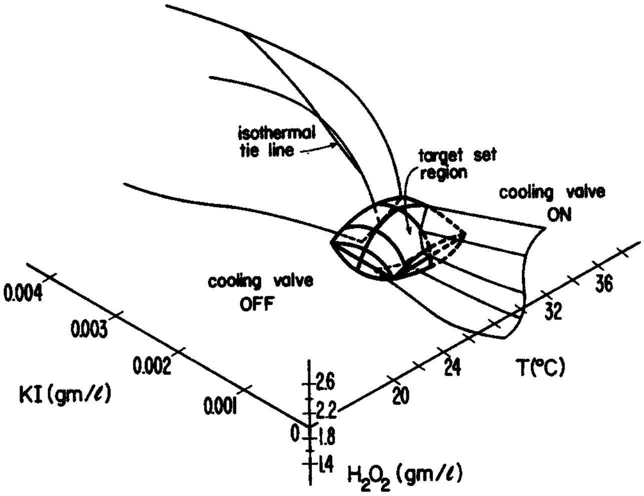

Fig. 4. Cooling valve switching surfaces.

$$\dot{\mathbf{p}} = -\frac{\partial H}{\partial \mathbf{x}} \tag{8}$$

The optimal control law resulting from maximizing the Hamiltonian is

$$u_1 = sgn\ (b_2 p_1) \tag{9}$$

$$u_2 = sgn\ (a_1 p_1 + a_2 p_2 + a_3 p_3) \tag{10}$$

and

$$b_2 = -\frac{(T - T_c)}{V_h \rho C_p} \tag{11}$$

$$a_1 = \frac{(T_0 - T)}{V_H} \tag{12}$$

$$a_2 = -\frac{C}{V_x} \tag{13}$$

$$a_3 = \frac{C_{KI_0} - C_{KI}}{V_x} \tag{14}$$

In order to compute this optimal control problem boundary conditions for the state and co-state variables must be specified. The target set which was chosen for this study is shown in Figure 2. For a trajectory to be time-optimal, it must lie on the boundary of the target set and the co-state vector is normal to a support hyperplane on the target set directed outward at the final time t_f (Hermes and LaSalle, 1969). With the co-state boundary condition established, the six state and co-state equations are integrated backwards in time starting from the surface of the target set and the optimal control law is given by Equations (9) and (10). By starting at various points on the target set, optimal switching surfaces can be developed and are shown in Figures 3 and 4. These switching surfaces define the bang-bang control algorithm for time-optimal control of a CSTR to the shown target set about the desired steady state operating condition. Once the target set is reached, single-loop proportional feedback control is used for each control variable. Temperature serves as the measured variable for coolant control and reaction rate for catalyst flow control.

EXTENDED KALMAN FILTER

A significant problem in applying optimal control to chemical processes is knowledge of all the process states. The problem is compounded by the fact that the system is subject to random disturbances. If we have a mathematical model of the process, a good idea of the intensity of the random disturbances and the degree of uncertainty in the measurements, then by applying the Extended Kalman Filter (Bryson and Ho, 1969; Hamilton et al., 1973; Wells, 1969) we can obtain optimal estimates of the measured variables and also optimal estimates of the entire state vector.

For a linear multistaged discrete-time system the optimal state estimates at a specific time interval i are

$$\hat{\mathbf{x}}_i = \bar{\mathbf{x}}_i + \mathbf{K}_i\,(\mathbf{m}_i - \mathbf{H}\,\bar{\mathbf{x}}_i) \tag{15}$$

where

$\bar{\mathbf{x}}_i$ are the states computed from the model equations,

$\mathbf{m}_i$ are the actual measured variables

and

$\mathbf{H}$ is the measurement matrix so that $\mathbf{H}\,\bar{\mathbf{x}}_i$ are the computed values for the measurement vector.

The recursive relationships for computing the Kalman Filter matrix $\mathbf{K}$ are

$$\mathbf{P}_i = \mathbf{M}_i - \mathbf{M}_i\mathbf{H}^T(\mathbf{H}\mathbf{M}_i\mathbf{H} + \mathbf{R})^{-1}\,\mathbf{H}\mathbf{M}_i \tag{16}$$

$$\mathbf{M}_{i+1} = \boldsymbol{\Phi}\mathbf{P}_i\boldsymbol{\Phi}^T + \boldsymbol{\Gamma}\mathbf{Q}\boldsymbol{\Gamma}^T \tag{17}$$

with

$$\mathbf{K}_i = \mathbf{P}_i\mathbf{H}^T\mathbf{R}^{-1} \tag{18}$$

Here $\mathbf{Q}$ is the covariance marix due to random noise in the state variables,

$\mathbf{R}$ is the covariance matrix due to random noise in the measured variables,

$\boldsymbol{\Phi}$ is the state transition matrix

and $\boldsymbol{\Gamma}$ is the noise disturbance transition matrix.

Equations (16) and (17) define the dynamic Kalman Filter. For large times, $t \to \infty$, the filter gains $\mathbf{K}_i$ approach a constant. Since the filter will be applied over many process time constants and also due to limited core storage on minicomputers used for the implementation of on-line estimation and control, the steady state version of the Kalman Filter is preferred. Here the recursive relations are computed off-line until constant or steady values of **M** and **P** are obtained. Using these constant values, the steady state Kalman Filter matrix **K** is then defined from Equation (18).

A discrete-time form of the system equations is obtained by using an Euler finite difference algorithm on Equation (7) to give

$$\bar{\mathbf{x}}_i = \hat{\mathbf{x}}_{i-1} + \Delta t\, \mathbf{f}(\hat{\mathbf{x}}_{i-1}, \hat{\mathbf{u}}_{i-1}) \tag{19}$$

Equation (19) can be placed in the linear discrete-time form needed for the Kalman Filter as

$$\bar{\mathbf{x}}_i = \mathbf{\Phi}\, \hat{\mathbf{x}}_{i-1} + \mathbf{\Gamma}\, \mathbf{d}_{i-1} \tag{20}$$

where the state transition matrix $\mathbf{\Phi}$ is

$$\mathbf{\Phi} = \left[\mathbf{I} + \frac{\partial \mathbf{f}}{\partial \mathbf{x}} \Delta t\right] \tag{21}$$

the expected value of the disturbance $\mathbf{d}_{i-1}$ is

$$E(\mathbf{d}_{i-1}) = \mathbf{0} \tag{22}$$

and

$$\mathbf{\Gamma} = \mathbf{I} \tag{23}$$

The measurement matrix for our CSTR control problem is given by

$$\begin{bmatrix} m_1 \\ \\ m_2 \end{bmatrix} = \begin{bmatrix} 1 & 0 & 0 \\ \dfrac{\partial m_2}{\partial x_1} & \dfrac{\partial m_2}{\partial x_2} & \dfrac{\partial m_2}{\partial x_3} \end{bmatrix} \begin{bmatrix} x_1 \\ x_2 \\ x_3 \end{bmatrix} \tag{24}$$

All partials are evaluated about the process steady states.

In order to apply the Extended Kalman Filter, we need to specify correct values for the covariance matrices. We assume that the cross correlation coefficients are small compared to auto correlation coefficients so that only the diagonal terms are significant in the covariance matrices. These diagonal terms correspond to expected variances in the state and measured variables. From data on the measured variables we have measured covariances of 0.003 for normalized temperature and 0.001 for deviation reaction rate. Thus

$$\mathbf{R} = \begin{bmatrix} .003 & 0 \\ 0 & .001 \end{bmatrix} \tag{25}$$

The work of Nyquist and Ramirez (1971) has demonstrated a modeling accuracy for this system within 3% when compared to experimental data. We therefore have a high degree of confidence in model predictions and consequentially used rather small values for the normalized model covariance terms. Values for **Q** were taken as

$$\mathbf{Q} = \begin{bmatrix} .001 & 0 & 0 \\ 0 & .001 & 0 \\ 0 & 0 & .001 \end{bmatrix} \tag{26}$$

The sampling time interval was chosen to be well within the dynamic time constants (10 min.) of the system [Equations (1), (2), and (3)] and not too small so as to commit the control computer to just sampling process instruments and not having time to perform other tasks. A sampling time of 12 seconds was used for this CSTR system. The steady state Kalman Filter Matrix thus computed is

$$\mathbf{K} = \begin{bmatrix} .43 & .0468 \\ .0069 & .405 \\ .00997 & .453 \end{bmatrix} \tag{27}$$

This Extended Kalman Filter was applied to a nonlinear simulation where the states were computed from the dynamic model equations with random noise (specified by **Q** and **R**) added to the measurement and state variables. The results showing the simulated filtered and simulated nonfiltered reaction rate measurements are given in Figure 5. The control variables are operated according to the time-optimal control law. Once the target set was reached, the control valves take on their steady state values. Even when the catalyst valve bumps on for a short duration due to errors in the polynomial curve-fitting of the switching surfaces, the optimal estimate of the reaction rate follows this dynamic forcing very well. The accuracy of the polynomial curve fits are within 1%. Figure 6 shows a comparison between the optimal estimates with noise for the two unmeasured states with their computed model values without noise. The agreement is excellent, showing that the Extended Kalman Filter based on a linearization is working very well in estimating unmeasured system states of the nonlinear model.

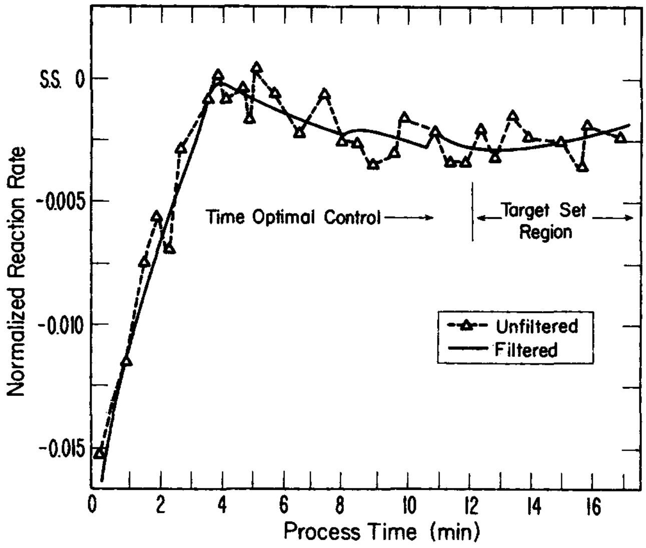

Fig. 5. Simulated filtered/unfiltered process reaction rate.

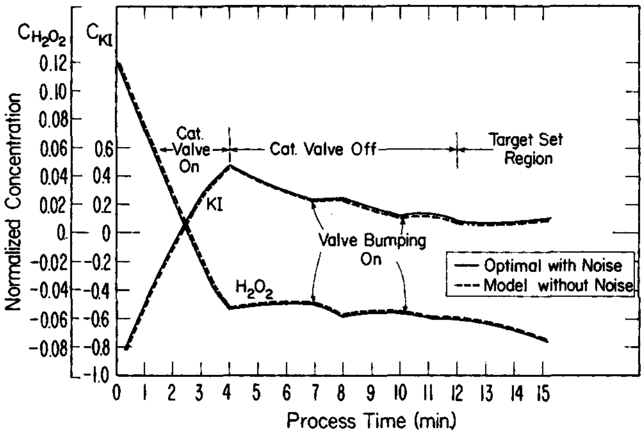

Fig. 6. Simulated response of KI and H_2O_2 concentrations.

IMPLEMENTATION OF REAL-TIME COMPUTER CONTROL

The time-optimal control and on-line filtering and estimation algorithms were implemented for this CSTR reactor using the CHEDACCS system (Chemical Engineering Data Acquisition and Control Computer System). The central processing unit for this minicomputer system is a Data General Corporation Nova 1210 series with 8K words of core memory and a real-time clock. The CHEDACCS configuration includes 32 variable gain analog inputs, 4 analog outputs, 16 relay-buffered digital outputs, 16 relay-

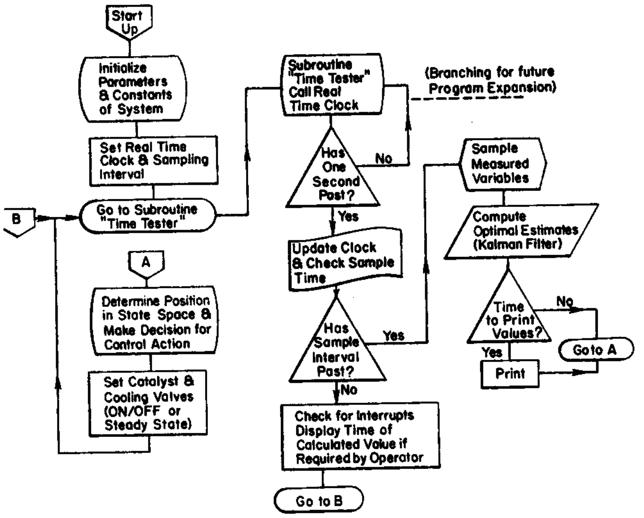

Fig. 7. Information flow diagram for real time control.

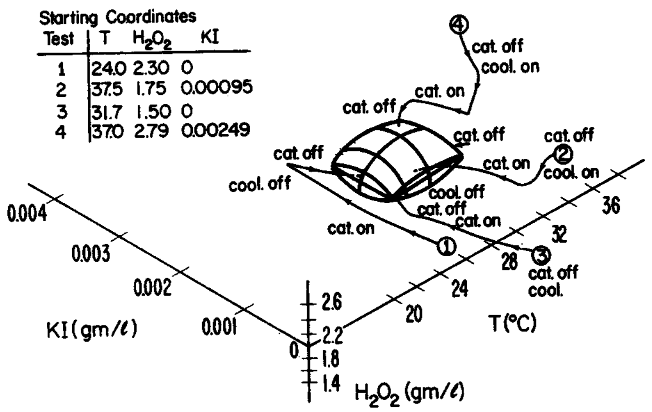

Fig. 8. Experimental trajectories of time-optimal control.

buffered digital inputs, a numerical keyboard and digital display, 16 illuminated push button switches, a high speed paper tape reader, and an ASR-33 teletype. The system language used to program this real-time control application was BASIC with real-time CALL extensions.

For this application, two analog to digital (A/D) channels were used for the reactor temperature and reaction rate inputs. Also two digital to analog (D/A) converters were used to control the catalyst flow valve and the coolant flow valve. Figure 7 shows a flow diagram for the computer program used to implement this real-time control and filtering problem. Details of the program and the hardware used can be found in the thesis by Lynch (1975).

EXPERIMENTAL RESULTS

Figure 8 shows the disturbances studied for this system. Two comparisons are made on the process states. The first compares the optimally estimated states with the measured states, that is, temperature and reaction rate with respect to time. This establishes the credibility of the Kalman Filter estimation method and tells us how well the model equations predict the dynamic changes in the experiment. The second comparison is the experimental estimated states with simulated estimated states. This comparison allows us to observe how well the computer-controlled experimental system is controlling the process in a time-optimal manner.

The comparison between measured and optimally estimated temperature profiles for two experiments are shown in Figures 10 and 11. Figure 9 gives the comparison of measured and optimally estimated rate data. The noise level in the rate data is significantly higher than that for temperature. Although there is a regular pattern to the rate noise data, we have treated it as white Gaussian noise for use in the Kalman Filter. The Kalman Filter does an excellent job in giving good estimates for both measured variables.

Figures 10 and 11 also give comparisons of simulated and experimentally estimated trajectories for two experimental tests. In Figure 10 we see that our actual real-time controlled system is performing almost exactly as our nonlinear simulated system under time-optimal control. However, Figure 11 shows a significant difference between the simulated and experimental response curves. The reason for this discrepancy is the fact that the coolant water temperature varied significantly during the actual experiment. Variations of 8°C were observed, but precise data was not taken. The model simulation assumed a constant value for this parameter, and therefore the simulated state variable estimates are not in agreement with the experimental state estimates that used actual measured data which reflect the changes that occurred in coolant water temperature. Note

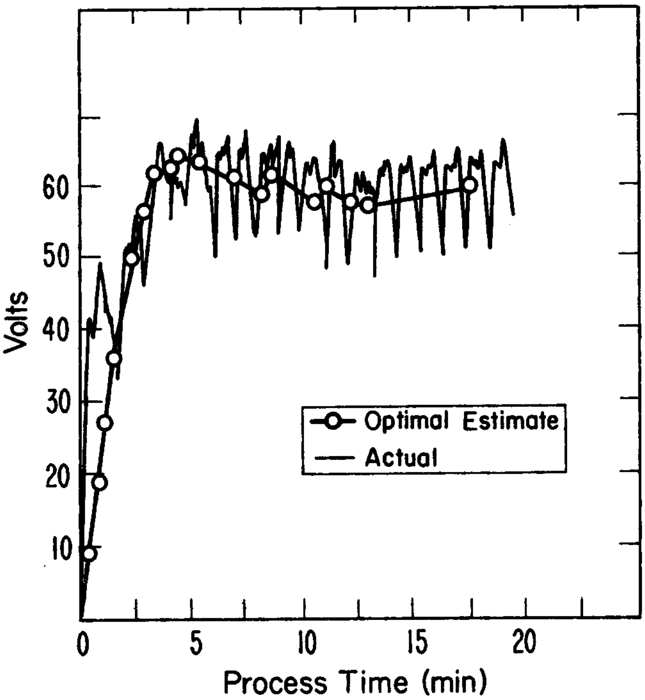

Fig. 9. Actual vs. optimally estimated reaction rate—Test 1.

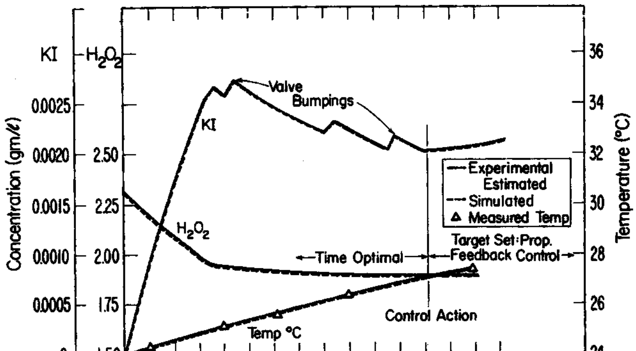

Fig. 10. Comparison of simulated and experimental trajectories—Test 1.

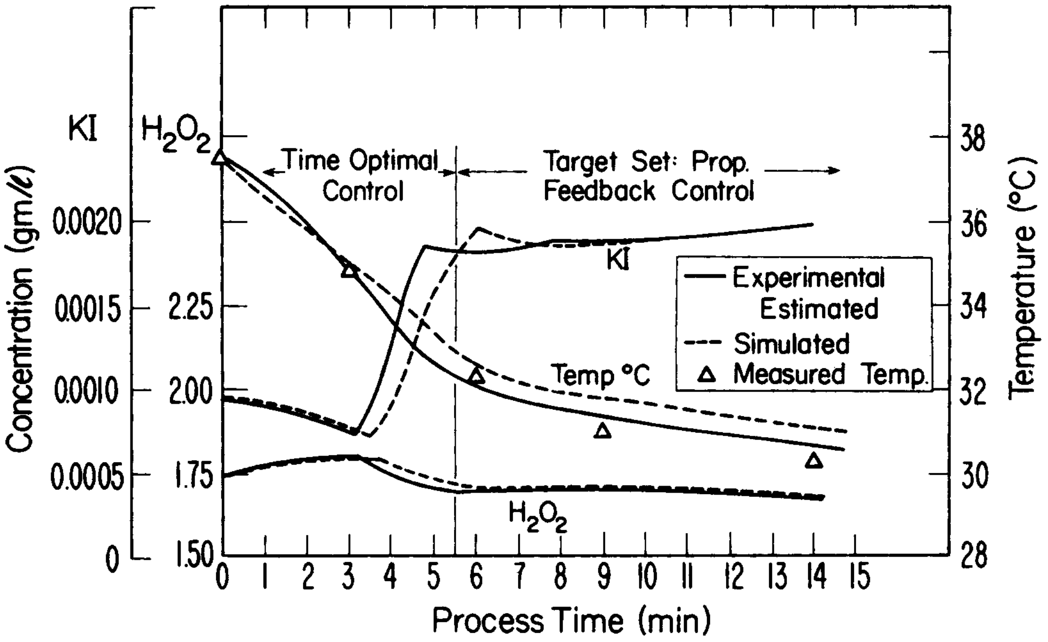

Fig. 11. Comparison of simulated and experimental trajectories—Test 2.

Table 3. Comparison of Control Policies

Initial temp., °C	Initial H_2O_2 conc., g mole/liter	Two-control variable time optimal	Time to reach target set One-control variable time optimal	Two-control variable proportional feedback
24	2.75	9.6 min	12.6 min	12.6 min
36.5	0.40	8.0	9.6	15.0
33	1.5	2.6	2.6	4.6
36.5	3.25	9.0	10.0	15.0

that the experimentally estimated value of temperature agrees well with that measured. This is an indication of the robustness of the Kalman Filter to unmeasured disturbances.

The purpose of this work was to demonstrate real-time multivariable time-optimal control of a stirred-tank reactor. It is important to compare this control scheme to on-line proportional feedback control. We have also considered the advantages, if any, of implementing a time-optimal control policy using two control variables when compared to the case with just the one control variable of coolant flow rate. Table 3 shows the results of comparing these three control schemes for four initial starting points. The two variable time-optimal control policy is significantly better (faster to reach the target set) than the one variable time-optimal policy which in turn is better than the proportional feedback policy using two control variables. In the proportional feedback control scheme temperature is the measured variable for coolant control and reaction rate the measured variable for catalyst flow control.

NOTATION

$\mathbf{B}$ = control matrix
C = hydrogen peroxide concentration, g mole/liter
C_{KI} = catalyst concentration, g mole/liter
C_p = heat capacity, cal/g °C
E = activation energy, cal/gmole
$\mathbf{f}$ = nonlinear functions given by the model equations
F = total feed rate, ml/min
F_{KI} = catalyst flow rate, ml/min
F_p = hydrogen peroxide feed rate, ml/min
$\mathbf{g}$ = nonlinear vector function
$\mathbf{H}$ = measurement matrix
$\mathbf{K}$ = Kalman Filter matrix
k_0 = frequency factor, 1/min
$\mathbf{m}$ = measured variable vector
$\mathbf{p}$ = co-state vector
Q_s = rate of heat due to stirring, cal/min
R = rate of reaction, gmoles/min
R' = gas constant, cal/g mole°C
t = time, min
T = temperature, °C
T_c = coolant temperature, °C
$\mathbf{u}$ = control vector
V_H = thermal reactor volume, cc
V_x = reaction volume, cc
$\mathbf{x}$ = state vector

Subscripts

i = discrete time interval $i(\Delta t)$
0 = input value
s = steady state value

Greek Letters

β = heat coil effectiveness factor
ρ = density

LITERATURE CITED

1. Athans, M., and P. L. Falb, *Optimal Control*, McGraw-Hill, New York (1966).
2. Bryson, Q. E., Jr., and Y. C. Ho, *Applied Optimal Control*, Blaisdell, Waltham, Mass. (1969).
3. Hamilton, J. C., D. E. Seborg, and D. G. Fisher, *AIChE J.*, **19**, 901 (1973).
4. Hermes, H., and LaSalle, *Function Analysis and Time-Optimal Control*, Academic Press, New York (1969).
5. Lynch, E. B., M.S. thesis, Univ. Colorado, Boulder (1975).
6. Nyquist, J. K., Ph.D. thesis, Univ. Colorado, Boulder (1970).
7. Nyquist, J. K., and W. F. Ramirez, *Chem. Eng. Sci.*, **26**, 1673 (1971).
8. Wells, C. H., 1969 JACC Reprints, p. 473, Boulder, Colorado (1969).

Manuscript received December 26, 1974; revision received April 3 and accepted April 4, 1975.